Journal of Institute of Control, Robotics and Systems (2013) 19(9):805-812
http://dx.doi.org/10.5302/J.ICROS.2013.13.9026 ISSN:1976-5622 eISSN:2233-4335

수중 기뢰 제거 로봇의 설계, 제어 및 위치 추정

Design, Control and Localization of Underwater Mine Disposal Robots

문 용 선, 고 낙 용*, 서 주 노
(Yong Seon Moon[1], Nak Yong Ko[2], and Joono Sur[3])
[1]Dept. Electronics Eng., Sunchon National University
[2]Dept. Control, Instrumentation, and Robot Eng., Chosun University
[3]Naval Systems R&D Center, Samsung Thales Co. Ltd.

Abstract: This paper describes the design, control, and localization which comprise major aspects of the development of underwater robots for the mine disposal. The developed robots are called the Mine Killer 1(MK-1) and MK-2. MK-1 had been developed from September 2009 and was presented at the 9-th International Symposium at NPS Monterey CA, on May 17-21, 2010[1]. The paper presents design of MK-1 and MK-2 in detail with comparison of these two versions of MKs. Then it derives hydrodynamic coefficients of MK-1. Based on the coefficients, the motion of MK-1 is simulated for straight line motion and circular motion. Also simulation results for PD control, LQ control and sliding mode control are presented. Finally, it shows a particle filter method for localization of the MK-1 and MK-2 using simple range data from acoustic beacons.

Keywords: mine disposal, underwater robot, hydrodynamic coefficient, control, location estimation, navigation

I. INTRODUCTION

UUVs (Unmanned Underwater Vehicles) such as AUVs (Autonomous Underwater Vehicles) and ROVs (Remotely Operated Vehicles) have been developed used for oceanographic observation, bathymetry, reconnaissance, exploration, biological monitoring, ocean engineering, and so on [2,3]. They have great potentials also for use in military and defense purposes. One of the promising uses is mine detection and disposal [4]. There have been several developments for this, such as SeaFox [5] and Minesniper [6].

One of the mine disposal methods using a UUV is that the UUV detects and carries the mine for disposal by other agent possibly human or autonomous system. Another method is that a UUV detects and approaches near to the mine, and the UUV itself finally explodes the mine. In this case, the UUV itself also explodes with the mine.

The MKs described in this paper are intended to explode with a mine. The MKs are equipped with camera and localization unit so that a human operator on a minesweeper can recognize the location of the robot and take visual image ahead of the robot. The robot approaches autonomously to the underwater mine whose location is already known and monitored by the operator. Once the robot gets near to the mine enough for the human operator to recognize the mine through camera image, the operator manually controls the MK and shoots a warhead to explode the mine.

This article presents development of MK-2 from the MK-1 whose design is presented at the 9-th symposium. Analysis of dynamics and application of control schemes for the MK-1 are addressed together with the design of MK-2 and a localization method tested for MKs. The localization uses range data from simple acoustic beacons and encoder data of the thrusters. The performance of the MK-2 is demonstrated at the 2011 Korea UUV conference on May 2011 both in a test tank and seashores. Since the MK is under development, the design and navigation of the MK requires extensive test and proof, and significant modification is expected. This article puts together partial results of the development processes together for up to date introduction to the MK development.

* 책임저자(Corresponding Author)
Manuscript received May 15, 2013 / revised June 10, 2013 / accepted June 30, 2013
문용선: 순천대학교 전자공학과(moon@urc.kr)
고낙용: 조선대학교 제어계측로봇공학과(nyko@chosun.ac.kr)
서주노: 삼성탈레스㈜ 해양시스템연구소(joono.sur@samsung.com)

Copyright© ICROS 2013

II. DESIGN OF MK-1 AND MK-2

1. Design of MK-1

MK-1 has four thrusters attached at the middle of the hull and four fins at the stern. These fins are fixed and don't control elevation or steering. Fig. 1 shows the structure of MK-1 and Table 1 summarizes the mechanical design.

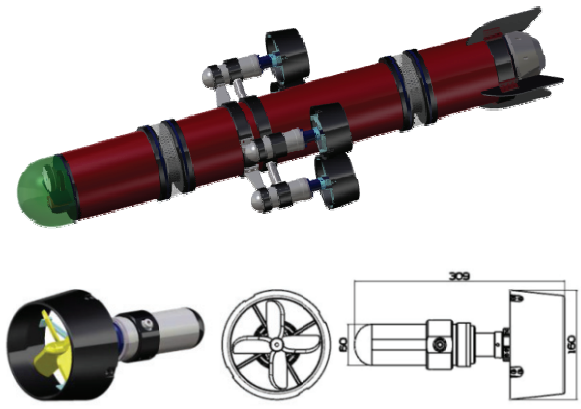

그림 1. MK-1의 구조와 구성 요소.
Fig. 1. Structure and components of the MK-1.

표 1. MK-1의 설계.
Table 1. Design of the MK-1.

Dimension	mm	1600 (length), 545 (width with thrusters), 340 (height with thrusters)
Weight	Kg	45
DOF		3(surge, pitch, yaw)
Hull material		Al 6061 T6/SUS 304
Number of thrusters		4

2. Design of MK-2

MK-2 has two horizontal thrusters, one vertical tunnel thruster, and balance control mechanism, while the MK-1 has four horizontal thrusters for actuation and maneuvering. It has the degree of freedom on the motion of surge, heave, yaw, and pitch, while the MK-1 lacks the mobility of heave. Fig. 2 shows the exterior and structure of the MK-2. The two horizontal thrusters control surge and yaw motion. The vertical thruster together with balance control mechanism in the hull controls the heave and pitch motion of the robot. This mechanism enables the robot hover around the mine while adjusting its heading for aiming and shooting.

The performance and design of the MK-2 are shown on the Table 2. Though the operation time for mine disposal is expected to be about 20 minutes, the endurance is set to be one and half hours for use with practice and drill.

The robot consists of three mechanical parts: the fore, middle, and stern. The fore has warhead, camera, light, and sensors for searching for and aiming at a mine. The middle has electronic devices and sensors for control, motor driving, and power management. It has also vertical tunnel thruster. Two thrusters are attached onto both sides of the middle. Balance control mechanism moves the battery pack back and forth to control the pitch of the robot. The stern has four fins which are fixed and enhances stable motion.

The thruster has a BLDC motor and duct. The BLDC motor has

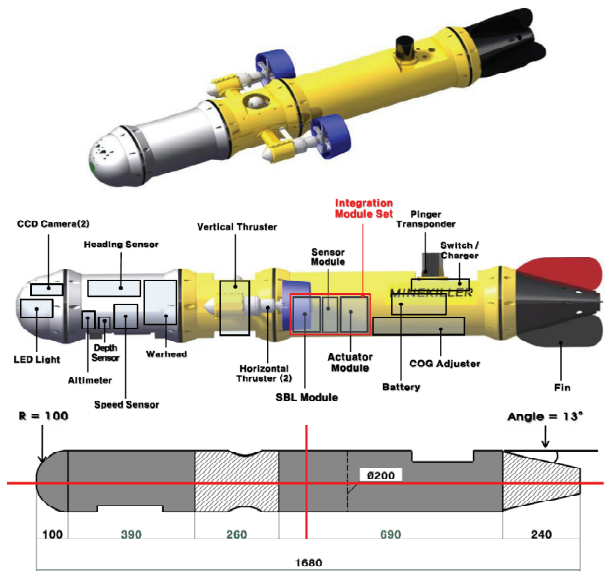

그림 2. MK-2의 구조와 구성 요소.
Fig. 2. Structure and components of the MK-2.

표 2. MK-2의 설계.
Table 2. Design of MK-2.

Dimension	mm	1680(length), 285(hull diameter), 580(width with thrusters)
Weight	Kg	45
DOF		4(surge, heave, yaw, pitch)
Depth of operation	m	100
Maximum speed	knots	7
Operation duration (endurance)	hours	1.5
Working Range	m	1,000
Battery		Li polymer, 24V 26Ah

200watts of power, 24V power supply, with 2,800 rpm of rated speed and 9A of rated current. A reduction gear of ratio 6:1 is used to enhance the torque to the rated torque of 680Nm. All the sensor modules and motor driver modules are connected to control electronics via the EtherCAT. This is the same feature as for the MK-1.

MK-2 is driven by network based motion and sensing controller. The EtherCAT also works for communication between the vehicle and the on-ship operation system through optical cable. Since the EtherCAT based control module allows high speed data transfer, the control unit can be located on-ship not in the MK. Most of the control strategy can be dealt with by the on-ship computer system. Since the robot is disposable and expendable, it is advantageous to make the vehicle as simple and inexpensive as possible. This architecture also helps to reduce power consumption of the robot.

III. HYDRODYNAMIC COEFFICIENTS AND CONTROL OF MK-1

1. Estimation of hydrodynamic coefficients

There are three major methods for estimation of hydrodynamic coefficients: experiment, use of CFD, and use of empirical formula. We used empirical formulas with analytical study. Though it doesn't yield the value as accurately as the experiment, it is useful for initial stage of study and rough assessment of the performance at low price and in short time. Since the KM-1 consists of a cylindrical hull, four thrusters, and four fins, we estimated the coefficients of these three parts separately considering the interaction between them.

Added mass coefficients of the hull are calculated using the strip method considering that the hull has slender body. The

표 3. MK-1의 유체역학 계수.
Table 3. Hydrodynamic coefficients of the MK-1.

(dimensional values)

coefficient	value	coefficient	value
L	1.494m	$Z_{\dot{w}}$	-64.32
D	0.2m	$Z_{\dot{q}}$	-1.67
M	47kg	$M_{\dot{w}}$	-1.67
$X_{\dot{u}}$	-2.35	$M_{\dot{q}}$	-11.52
$Y_{\dot{v}}$	-64.32	$K_{\dot{p}}$	-1.03
$Y_{\dot{r}}$	1.67	X_u	-4.7
$N_{\dot{v}}$	1.67	Y_v	-144.8
$N_{\dot{r}}$	-11.52		

coefficient for the fin is calculated using the method of [7]. As for the thruster, it is approximated as a cylinder. Damping coefficient for the hull is calculated using the method of DATCOM [8]. For the damping coefficient of the fin, [7] is used. Some of the hydrodynamic coefficients are shown on the Table 3. The notations are adopted from those of SNAME [9,10].

2. Simulation of the MK-1 motion

The system is modeled according to the conventional dynamic modeling of Fossen [9] with the notations adopted from SNAME [10]. The motion of the MK-1 is simulated using MatLab. For the straight line motion test, the thrust force of 150N is applied to all of the four thrusters, $T_1 = T_2 = T_3 = T_4 = 150N$. Fig. 3 shows the thruster arrangement and the center of gravitational and buoyant force. In this figure "B" denotes buoyant force, and "W" does the gravitational force. For the simulation, initial velocity of $u = 2m/sec$ is assumed. Fig. 4 shows the trajectory of the motion. In 200 sec, MK-1 moved to the distance of 400m corresponding to the 3.9 knots of speed.

If thrust force of $T_1 = T_2 = 150N$ and $T_3 = T_4 = 145N$ is applied, MK-1 moves straight with the pitch angle of 2.5 degrees. This is because at the pitch angle of 2.5 degrees, the torque by the difference of thrust force becomes the same as that induced by the difference of center of gravity and center of buoyancy which is located over the center of gravity. Fig. 5 shows the simulated motion by torque induced by thrust force difference. At the initial stage of the motion there shows some oscillatory unstable motion in pitch angle as shown in the Fig. 5(a).

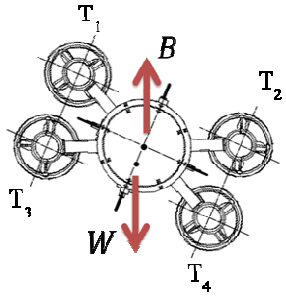

그림 3. 추진기 배치, 중력 중심과 부력 중심 (후방에서 본 그림).

Fig. 3. Thruster arrangement and center of gravitational and buoyant force (view from the back).

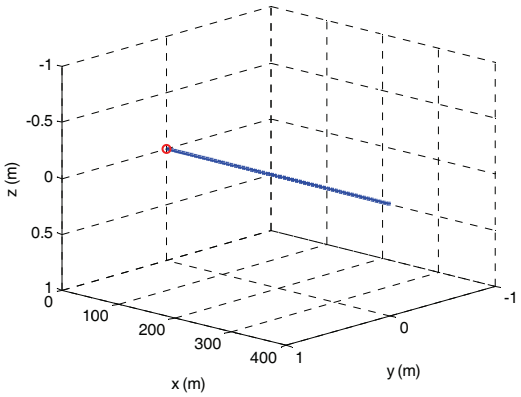

그림 4. 균일하게 분배된 추진력들에 의한 직선 운동.

Fig. 4. Straight line motion with equally distributed thrust force.

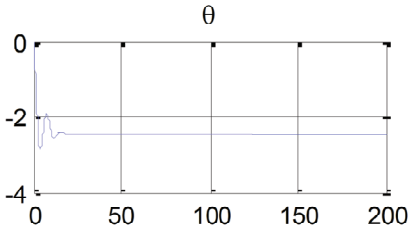

(a) Pitch angle with time.

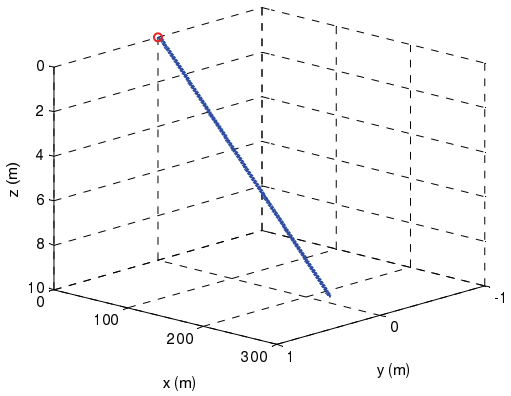

(b) Trajectory of the MK-1.

그림 5. 추진력 차이에 의해 발생하는 운동과 토오크.

Fig. 5. The motion with torque caused by thrust force difference.

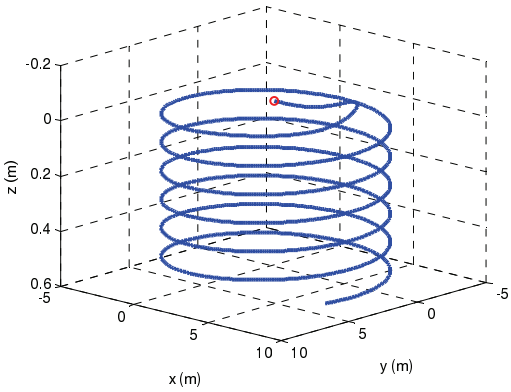

(a) Motion by z directional torque.

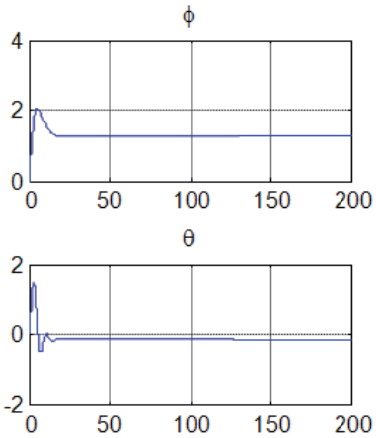

(b) Roll and pitch by z directional torque(horizontal axis: time in sec.).

그림 6. 추진력 $T_1 = T_3 = 150N$ 과 $T_2 = T_4 = 145N$ 에 의해 발생하는 운동 궤적과 피치각 및 요각.

Fig. 6. Motion trajectory and the angle of pitch and yaw by the thrust of $T_1 = T_3 = 150N$ and $T_2 = T_4 = 145N$.

The final simulation verifies yaw motion generated by z-directional torque. The thrust force of $T_1 = T_3 = 150N$ and $T_2 = T_4 = 145N$ is applied. Fig. 6 shows the motion trajectory, roll and pitch. The thrusters are located ahead of gravitational center, and the gravitational center is located below the center of the hull. This causes temporary upward trajectory at the initial stage of motion. It is notable that it develops pitch angle which brings the vehicle to dive gradually into 0.5 m depth in 200 seconds. The radius of circulation is 6m approximately.

3. Simulation of controlled motion

Control law of PD, LQ, and sliding mode control is applied to drive the robot to the depth of 3m from the initial depth of zero. The PD control law uses the equation (1).

$$u = K^{\theta}{}_{P}\tilde{\theta} + K^{\theta}{}_{D}\dot{\tilde{\theta}} + K^{z}{}_{P}\tilde{z} + K^{z}{}_{D}\dot{\tilde{z}} \tag{1}$$

$K^{\theta}{}_{P}$, $K^{\theta}{}_{D}$, $K^{z}{}_{P}$, and $K^{z}{}_{D}$ are the proportional control gain and derivative control gain for the control of pitch θ and depth z respectively. Fig. 7 shows simulated vehicle trajectory and the thrust forces required for the motion.

For the LQ control, the system is linearized as the following.

$$\dot{x} = Ax + Bu, x = [w, q, \theta, z]^T \tag{2}$$

$$A = \begin{bmatrix} m - Z_{\dot{w}} & -mx_G - Z_{\dot{q}} & 0 & 0 \\ -mx_G - M_{\dot{w}} & I_y - M_{\dot{q}} & 0 & 0 \\ 0 & 0 & 1 & 0 \\ 0 & 0 & 0 & 1 \end{bmatrix}^{-1} \begin{bmatrix} Z_w & mu_0 + Z_q & 0 & 0 \\ M_w & -mx_G u_0 + M_q & -mg\overline{BG}_z & 0 \\ 0 & 1 & 0 & 0 \\ 1 & 0 & -u_0 & 0 \end{bmatrix}$$

$$B = \begin{bmatrix} 0 & 0 \\ -x_{th2} & x_{th2} \\ 0 & 0 \\ 0 & 0 \end{bmatrix}, \qquad u = [T_1 + T_2 \quad T_3 + T_4]^T$$

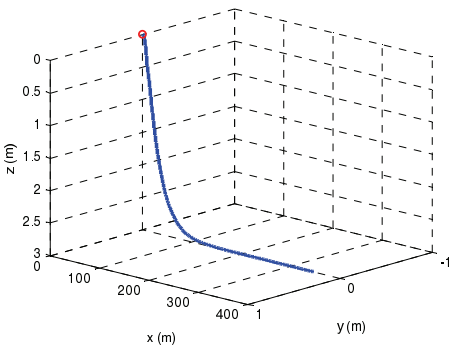

(a) Trajectory by PD control.

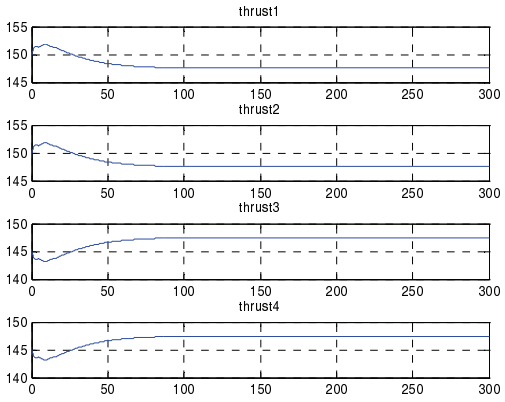

(b) Controlled thrust force for the motion.

그림 7. PD 제어에 의한 운동 궤적과 추진력.

Fig. 7. Motion trajectory and thrust forces for the PD control.

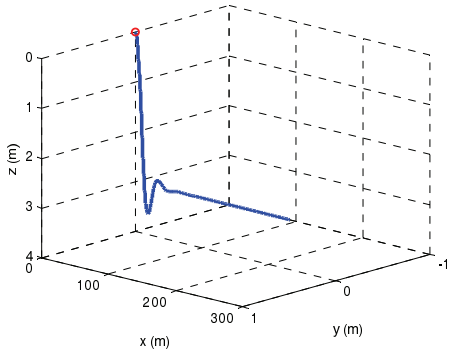

(a) Trajectory of the motion by LQ control.

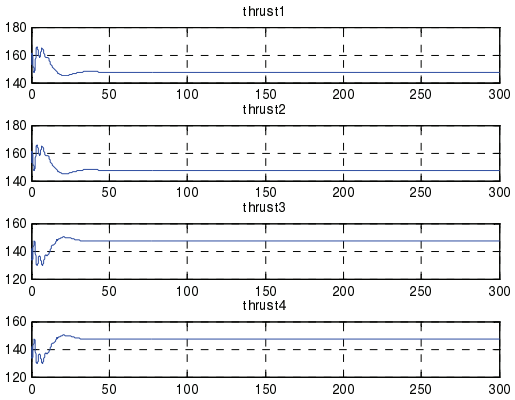

(b) Controlled thrust forces.

그림 8. LQ 제어에 의한 운동 궤적과 추진력.

Fig. 8. Motion trajectory and thrust forces for the LQ control.

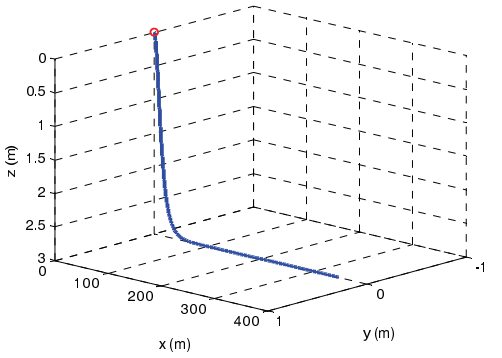

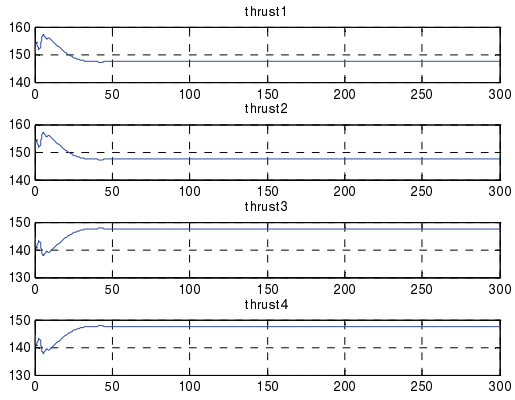

그림 9. 슬라이딩 모드 제어에 의한 운동 궤적과 제어 추진력.

Fig. 9. Motion trajectory and controlled thrust forces in case of sliding mode control.

The LQ control law minimizes the following cost function.

$$J(x_0, u) = \int_0^\infty (x^T Q x + u^T R u) dt \quad (3)$$

$$u(t) = -R^{-1} B^T P x \quad (4)$$

P satisfies the Riccati equation.

$$A^T P + PA + PBR^{-1}B^T P + Q = 0 \quad (5)$$

Fig. 8 depicts the LQ control result driven by simulation.

Sliding mode control which is appropriate for nonlinear system is applied for the MK-1. The equation (6) is used as the sliding surface.

$$\sigma = s^T \tilde{x} \quad (6)$$

$\tilde{x}$ represents estimation error, s does the sliding surface coefficient, and σ does the sliding surface. As σ converges to zero, so does the estimation error $\tilde{x}$. To make the σ converge to zero, control input is set to be the following.

$$u(t) = [s^T b]^{-1}\left[-s^T Ax(t) - s^T \hat{f}(t) + s^T \dot{x}_{com}(t) - \eta tanh(\sigma(t)/\varphi)\right] \quad (7)$$

Fig. 9 shows the result of sliding mode control simulated using MatLab.

IV. LOCATION ESTIMATION FOR NAVIGATION

Estimation of the vehicle location is essential for navigation and control. A particle filter(PF) based localization method(often called the MCL, Monte Carlo Localization) is used for the MKs and tested through simulation and experiment in a test pool [11,12].

1. Monte Carlo Localization

The algorithm of MCL is described on the Table 4. The method represents robot location probabilistically using particles. The method applies every time the robot detects measurements. In our research, the measurement indicates distances from acoustic beacons. In the algorithm, X_t represents a set of M particles which represent possible locations of the robot at time t. z_t is the distances from acoustic beacons, and u_t is the motion information measured by proprioceptive sensors such as encoders of the thrusters. E represents the locations of the acoustic beacons.

표 4. MK-1과 MK-2의 몬테 카를로 위치 추정.
Table 4. Monte Carlo localization for the MK-1 and MK-2.

PF method$(X_{t-1}, \boldsymbol{u}_t, \boldsymbol{z}_t, E)$	
1.	$\overline{X_t} = X_t = \phi$
2.	*for* $i = 1$ *to* M *do*
3.	$\boldsymbol{x}_t^{[i]} = Motion\ model(\boldsymbol{u}_t, \boldsymbol{x}_{t-1}^{[i]})$
4.	$\omega_t^{[i]} = Sensor\ model(\boldsymbol{z}_t, \boldsymbol{x}_t^{[i]}, E)$
5.	*endfor*
6.	*for* $i = 1$ *to* M *do*
7.	$\boldsymbol{x}_t^{[i]} = Resampling\left(\left\{\left(\boldsymbol{x}_t^{[i]}, \omega_t^{[i]}\right) \middle\| j = 1, \cdots, M\right\}\right)$
8.	*endfor*
9.	*return* X_t

Line 3 of the Table 4 depicts the prediction step which calculates a possible location of a particle based on dead-reckoning. Line 4 assigns belief to each predicted particle using measured sensor data. In our research, the data for belief calculation is the range data from acoustic beacons to the robot. Lines 6 to 8 resamples possible locations form the predicted particles to provide corrected possible locations. Therefore, these

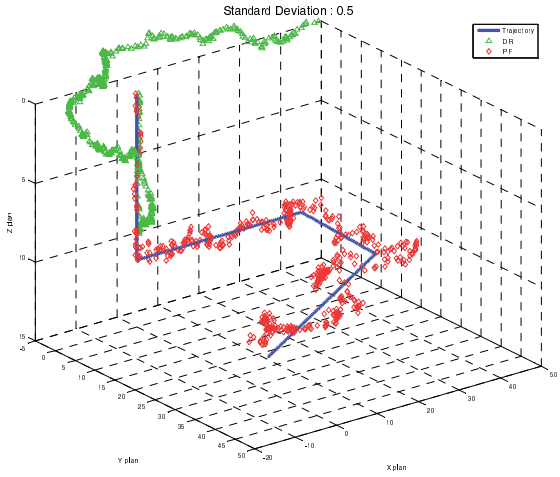

(a) PF result for the case of standard deviation $\sigma = 0.5$.

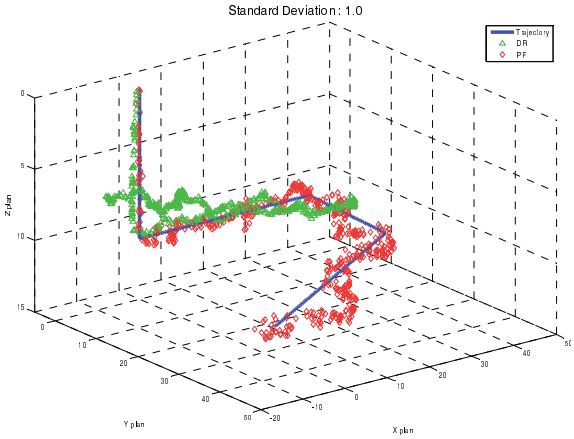

(b) PF result for the case of standard deviation $\sigma = 1.0$.

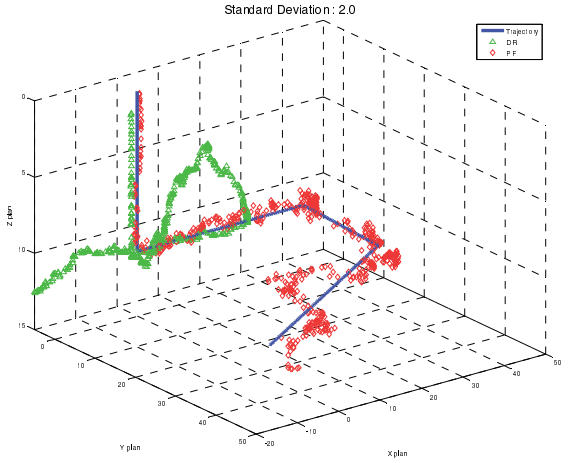

(c) PF result for the case of standard deviation $\sigma = 2.0$.

그림 10. PF 방법에 의한 위치 추정 결과.
Fig. 10. Location estimation result of the PF method.

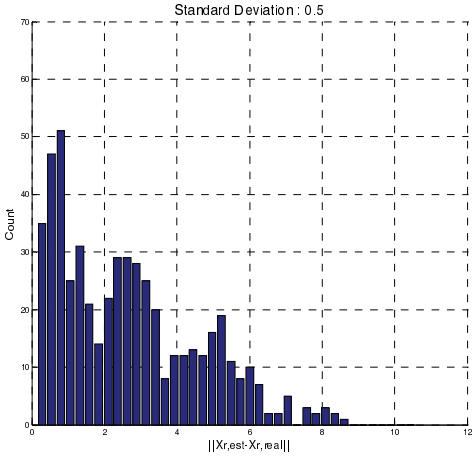

(a) Localization error distribution with the case of $\sigma = 0.5$.

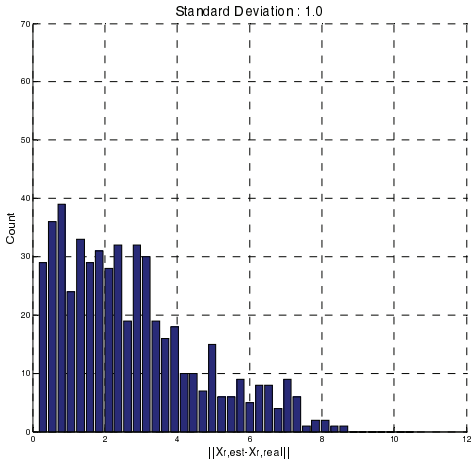

(b) Localization error distribution with the case of $\sigma = 1.0$.

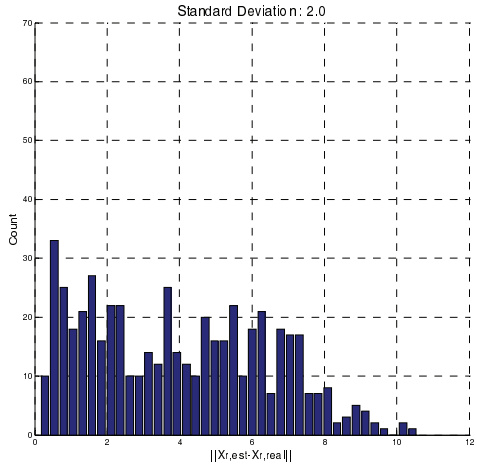

(c) Localization error distribution with the case of $\sigma = 2.0$.

그림 11. 측정 불확실성에 의한 위치 추정 오차 분포의 비교.
Fig. 11. Comparison of error distribution in relation to measurement uncertainty.

lines correspond to the correction step and complete an iteration of the MCL algorithm.

2. Localization using TDOA (Time Difference of Arrival)

The MCL is tested using simulation. The simulation uses five acoustic beacons from which four TDOA (Time Difference of Arrival) data are obtained. The performance of the PF degrades as the measurement error increases. Fig. 10(a), (b), and (c) shows the location estimation results with standard deviation of the range measurement error σ = 0.5, 1.0, and 2.0 respectively.

In the Fig. 10, the blue line indicates the robot trajectory and the red circles show the result by MCL, while the green circles do the result by dead-reckoning using only the encoder data of the thrusters. Comparing (a), (b), and (c) reveals that measurement with lower uncertainty with lower standard deviation of measurement noise provides more accurate location estimation.

Fig. 11 shows the error distribution of localization of PF method. It indicates that less uncertainty of the range measurement yields more accurate estimation of location. With lower uncertainty, the localization error concentrates within narrower range while higher uncertainty yields broader distribution of the localization error. It is noticeable that in the case of $\sigma = 2.0$, the error reaches over to 10.0m and the significant portion of the error lies over the error range of 6.0m.

3. Localization using TOA

The algorithm of MCL is tested through experiments in a test tank in the National Fisheries Research and Development Institute at Pusan, shown in the Fig. 12. The experiment uses 2 pingers for acoustic signal transmission and a hydrophone attached to the robot. Fig. 13 shows the configuration for the experiment. The robot travels between two way points $P_1(0,0,1)$m and $P_2(15,0,1)$m whose coordinates are represented according to the standard coordinates used for marine vehicles by Society of Naval Architecture and Marine Engineers [10].

The method uses 1,000 particles, and the estimated locations which are the average of these particle locations are shown in the Fig. 14. The estimation error at the way point P_1 and P_2 is shown in the Table 5 and Table 6 respectively. The maximum error distance from the way points is 1.4428m at the way point

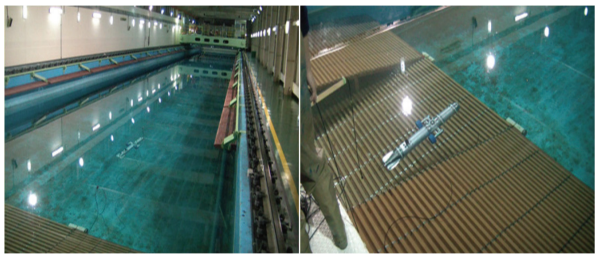

그림 12. 실험용 예인 수조와 수중 로봇.
Fig. 12. Towing tank and the underwater robot for the experiment.

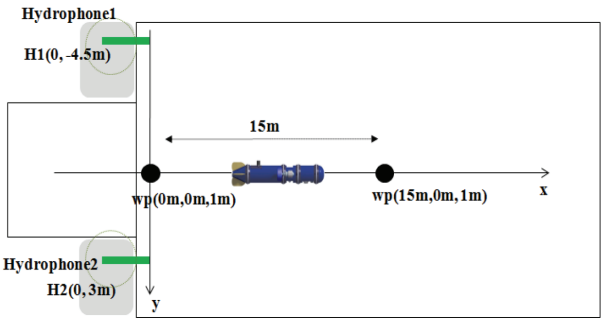

그림 13. 실험을 위한 환경 설정.
Fig. 13. Configuration for the experiment.

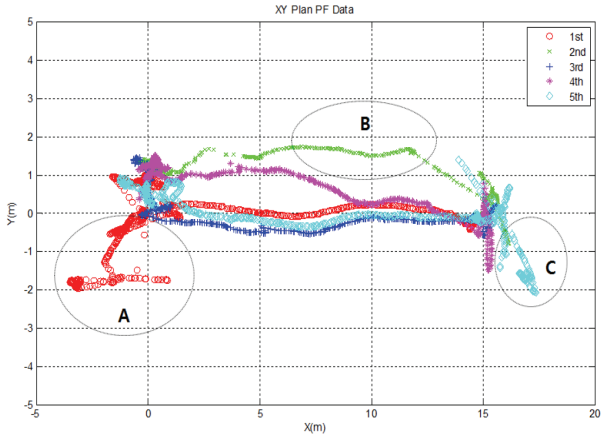

그림 14. 추정된 xy 평면에서 궤적.

Fig. 14. Estimated trajectory in the xy plane.

표 5. 경유점 P_1에 대해 추정된 위치(단위: m).

Table 5. Estimated location for the way point P_1(unit: m).

	x	y	z	error
2nd	-0.32892	1.35421	0.626474	1.4428
4 th	-0.25793	0.563906	0.597935	0.7390

표 6. 경유점 P_2에 대해 추정된 위치(단위: m).

Table 6. Estimated location for the way point P_2(unit: m).

	x	y	z	error
1 st	14.7437	-0.18066	0.898906	0.3295
3 rd	15.2773	-0.41532	0.750819	0.5581
5 th	14.757	-0.11727	0.374185	0.6815

P_1. The trajectory between these two way points is not controlled straight since the experiment concentrated on the repeatability of the estimation at the way points. So, the estimated locations between the waypoints are irrelevant to the performance of the localization performance of the proposed method. Since the robot doesn't have the mobility of pure turn with no linear motion, the trajectory shows back and forth motion at the way points. The location estimation by the MCL is much better than that by the dead-reckoning which uses only the data of thruster encoders.

V. CONCLUDING REMARKS AND FURTHER RESEARCH

This paper describes design, control, and localization of the underwater mine disposal robot MK-1 and MK-2. The mechanical design is described which implements surge, pitch, yaw, and heave motion. Along with the hydrodynamics coefficients, simulation results of control by PD, LQ, and sliding mode control law are presented. Also, localization using MCL is tested in a test tank navigation experiment. The above composes major aspects of development of a UUV for mine disposal.

The MKs will be incorporated with a navigation system and minesweeper. Incorporation of intensive works on obstacle avoidance and control is needed [13,14]. One of the problems to be solved is how to reduce the adverse effect by the tether. As the range of the work space increases, the drag force by the tether also increases. This pulls the robot back and reduces the controllability of the MK-2. Also, the tether may tangle as the robot moves back and forth. Since the acoustic communication is slower and less reliable than the wired communication through tether, it is inevitable to use tether for remote control at the final stage of aiming and shooting. The final goal of our project is to develop a UUV for mine disposal which works autonomously from the onset to the final explosion with as little intervention as possible through acoustic communication without tether.

REFERENCES

[1] Y. S. Moon, N. Y. Ko, J. Sur, and Y. O. Lee, "Development of Torpedo Type Mine Disposal Robot RUCUR MK-1," *Proc. 9th Int. Symp. Technology and the Mine Problem Series*, Monterey, May 17-21, 2010.

[2] S. B. Williams, et al., "Monitoring of benthic reference sites: using an autonomous underwater vehicle," *IEEE Robotics & Automation Magazine*, vol. 19, no. 1, pp. 73-84, Mar. 2012.

[3] F. Song, P. E. An, and A. Folleco, "Modeling and simulation of autonomous underwater vehicles: design and implementation," *IEEE Journal of Oceanic Engineering*, vol. 28, no. 2, pp. 283-296, Apr. 2003.

[4] S. Sariel, T. Balch, and N. Erdogan, "Naval mine countermeasure missions," *IEEE Robotics & Automation Magazine*, vol. 15, no. 1, pp. 45-52, Mar. 2008.

[5] W. Hornfeld, "Status of the atlas Elektronik's modular AUV family," *Proc. 25th International Conference on Offshore Mechanics and Arctic Engineering*, vol. 1, pp. 707-715, Hamburg, Germany, June, 2006.

[6] A. Lovik, A. R. Bakken, J. Dybedal, T. Knudsen, and J. Kjoll, "Underwater protection system," *Proc. of OCEANS 2007*, pp. 1-8, 2007.

[7] Lewis, Edward V., *Principles of Naval Architecture*, vol. 3, Society of Naval Architects and Marine Engineers, 1989.

[8] E. P. Holmes, "Prediction of hydrodynamic coefficients utilizing geometric considerations," Master's thesis, Naval Postgraduate School, Monterey CA, 1995.

[9] T. I. Fossen, *Guidance and Control of Ocean Vehicles*, John Wiley and Sons, 1995.

[10] Hydromechanics Subcommittee, Society of Naval Architects and Marine Engineers (U.S.), *Nomenclature for Treating the Motion of a Submerged Body Through a Fluid*, Technical and Research Bulletin, no. 1-5, 1950.

[11] N. Y. Ko, T. G. Kim, and Y. S. Moon, "Particle filter approach for localization of an underwater robot using time difference of arrival," *Proc. of OCEANS 2012*, May 2012, Yeosu Korea.

[12] N. Y. Ko, T. G. Kim, and S. W. Noh, "Monte carlo localization of underwater robot using internal and external information," *Proc. 2011 IEEE Asia -Pacific Services Computing Conference*, pp. 410-415, Jeju, Dec. 2011.

[13] D. Lee, H. W. Kim, and J. Lee, "Obstacle recognition and avoidance of the bio-mimetic underwater robot using IR and compass sensors," *Journal of Institute of Control, Robotics and Systems (in Korean)*, vol. 18, no. 10, pp. 895-987, Oct. 2012.

[14] H. Shim, B. Jun, and P. Lee, "Dynamic workspace control of underwater manipulator considering ROV motion," *Journal of Institute of Control, Robotics and Systems (in Korean)*, vol. 17, no. 5, pp. 397-511, May 2011.

Yong Seon Moon

1983 Bachelor, Dept. Electronics Eng., Chosun University. 1985 Master, Dept. Electronics Eng., Chosun University. 1989 Ph.D., Dept. Electronics Eng., Chosun University. 1992~present. Professor, Dept. Electronics Engineering, Sunchon National Univ. Research area robot network and safety.

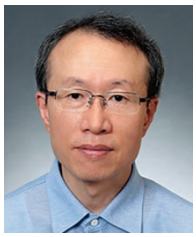

Nak Yong Ko

1985 Bachelor, Dept. Control and Instrumentation Eng., Seoul National University. 1987 Master, Dept. Control and Instrumentation Eng., Seoul National University. 1993 Ph.D., Dept. Control and Instrumentation Eng., Seoul National University. 1997~1998, 2004~2005 Visiting research, Robotics Institute, Carnegie Mellon Universty. 1992~present. Professor, Dept. Control, Instrumentation, and Robot Engineering, Chosun Univ. Research interests navigation of underwater vehicles, navigation of robots indoors and outdoors

Joono Sur

1981, 1985 B.S. degree in Mechanical Engineering, Naval Academy and Seoul National University, Korea. 1989 M.S. degree in Mechanical Engineering, Naval Postgraduate School, USA. 1997 Ph.D. degree in Mechanical Engineering, University of California at Santa Babara, USA. 1997~2011 faulty of Mechanical Engineering, Naval Academy. 2011~present Naval System R&D Center, Samsung Thales Co. Ltd. Research interests control, navigation, and autonomy of unmanned system.